



A machine learning approach relating 3D body scans to body composition in humans

James D. Pleuss¹ · Kevin Talty¹ · Steven Morse¹ · Patrick Kuiper¹ · Michael Scioletti¹ · Steven B. Heymsfield ² · Diana M. Thomas ¹

Received: 30 August 2018 / Accepted: 5 September 2018
© Springer Nature Limited 2018

Abstract

A long-standing question in nutrition and obesity research involves quantifying the relationship between body fat and anthropometry. To date, the mathematical formulation of these relationships has relied on pairing easily obtained anthropometric measurements such as the body mass index (BMI), waist circumference, or hip circumference to body fat. Recent advances in 3D body shape imaging technology provides a new opportunity for quickly and accurately obtaining hundreds of anthropometric measurements within seconds, however, there does not yet exist a large diverse database that pairs these measurements to body fat. Herein, we leverage 3D scanned anthropometry obtained from a population of United States Army basic training recruits to derive four subpopulations of homogenous body shape archetypes using a combined principal components and cluster analysis. While the Army database was large and diverse, it did not have body composition measurements. Therefore, these body shape archetypes were paired to an alternate smaller sample of participants from the Pennington Biomedical Research Center in Baton Rouge, LA that were not only similarly imaged by the same 3D scanning machine, but also had concomitant measures of body composition by dual-energy X-ray absorptiometry body composition. With this enhanced ability to obtain anthropometry through 3D scanning quickly of large populations, our machine learning approach for pairing body shapes from large datasets to smaller datasets that also contain state-of-the-art body composition measurements can be extended to pair other health outcomes to 3D body shape anthropometry.

Introduction

Anthropometric measures in adult humans have been used for centuries to quantify and categorize body types and shapes [1]. In more recent history, indices formulated by algebraic combinations of anthropometric measurements such as the body mass index (BMI) have been experimentally correlated to percent body fat and other components of body composition [2–5]. These indices [6–8] rely on manual measurements that are relatively simple to obtain in

large-scale epidemiology studies or through national health surveys [5, 9]. However, manual measurements are prone to inter-rater reliability error, are labor intensive, and are restrictive in scope, i.e., limited to what is feasible to quickly measure [10, 11].

The advent of three-dimensional (3D) body image scanning technology has increased our capacity to obtain an extraordinary number of accurate body measures within seconds [12–15]. These 3D scanned anthropometry measurements have been validated against carefully collected manual measurements [12, 13]. However, pairing data obtained from 3D body imaging scanning technology to adiposity and other body composition outcomes remain challenging. Such a study requires a research facility with access to a 3D body image scanner and an accurate body composition measurement technology such as the dual-energy X-ray absorptiometry (DXA) or magnetic resonance imaging. Even with access to such equipment, research facilities still will likely recruit participants from the regional location of the facility.

Electronic supplementary material The online version of this article (<https://doi.org/10.1038/s41430-018-0337-1>) contains supplementary material, which is available to authorized users.

✉ Diana M. Thomas
diana.thomas@usma.edu

¹ Department of Mathematical Sciences, United States Military Academy, West Point, NY, USA

² Pennington Biomedical Research Center, Baton Rouge, LA, USA

The Leipzig Research Center for Civilization Diseases in Leipzig, Germany has been developing a database that consists of 3D body human body image scans in local residents acquired through the Human Solutions technology since 2011 [16]. From this data, Löffler-Wirth et al. [16] applied machine learning to identify 13 different body shape archetypes from this data. Löffler-Wirth et al. [16] apply a neural network approach called self-organizing maps to transform this high-dimensional 3D data to low-dimensional representations in the form of body shape archetypes that can be visualized.

Here we add to the work in [16] threefold. Our Human Solutions database, which was acquired from Human Solutions 3D body image scans employed by the United States Army for the purpose of automatic and accurate uniform sizing in basic training recruit, is racially and geographically diverse. The United States Army represents the largest branch of the United States military and employs Soldiers from all 50 states [17]. Forty-three percent of active duty personnel are non-white race/ethnicities and 17% are female [18].

Second, we combine a principal component analysis (PCA) and cluster analysis (CA) to develop four homogenized populations that represent distinct body shape archetypes. As pointed out in [16], PCA alone or CA alone does not outperform self-organized maps, however, the application of these techniques in sequence can reduce the number of archetype subpopulations. Identification of these archetypes then allows us to pair body composition measurements from a separate and smaller database to them.

Finally, a smaller sample of Human Solutions scanned participants from the Pennington Biomedical Research Center (PBRC) in Louisiana were assigned to their respective body shape archetypes. These PBRC participants also had DXA measured body composition, which then could be analyzed within each body shape archetype. Our method of using descriptive data algorithms like PCA and CA to homogenize subpopulations and then pair to health outcomes can be utilized in the nutrition field to relate conclusions from “big data” to smaller datasets that contain measurements that are much more challenging or expensive to collect.

Methods

Study design

There were three main questions this study was designed to address. (1) Are there natural quantifications of collinearities within the 3D imaged body shape measures? For example, it is known that limb length and height are strongly correlated [19, 20]. We seek the pairwise strength

of the correlations between all of the body measures. (2) Do body shapes aggregate into distinct subpopulations; that is, are there archetype body shapes that can be algorithmically identified? (3) How does body composition differ between the archetypes?

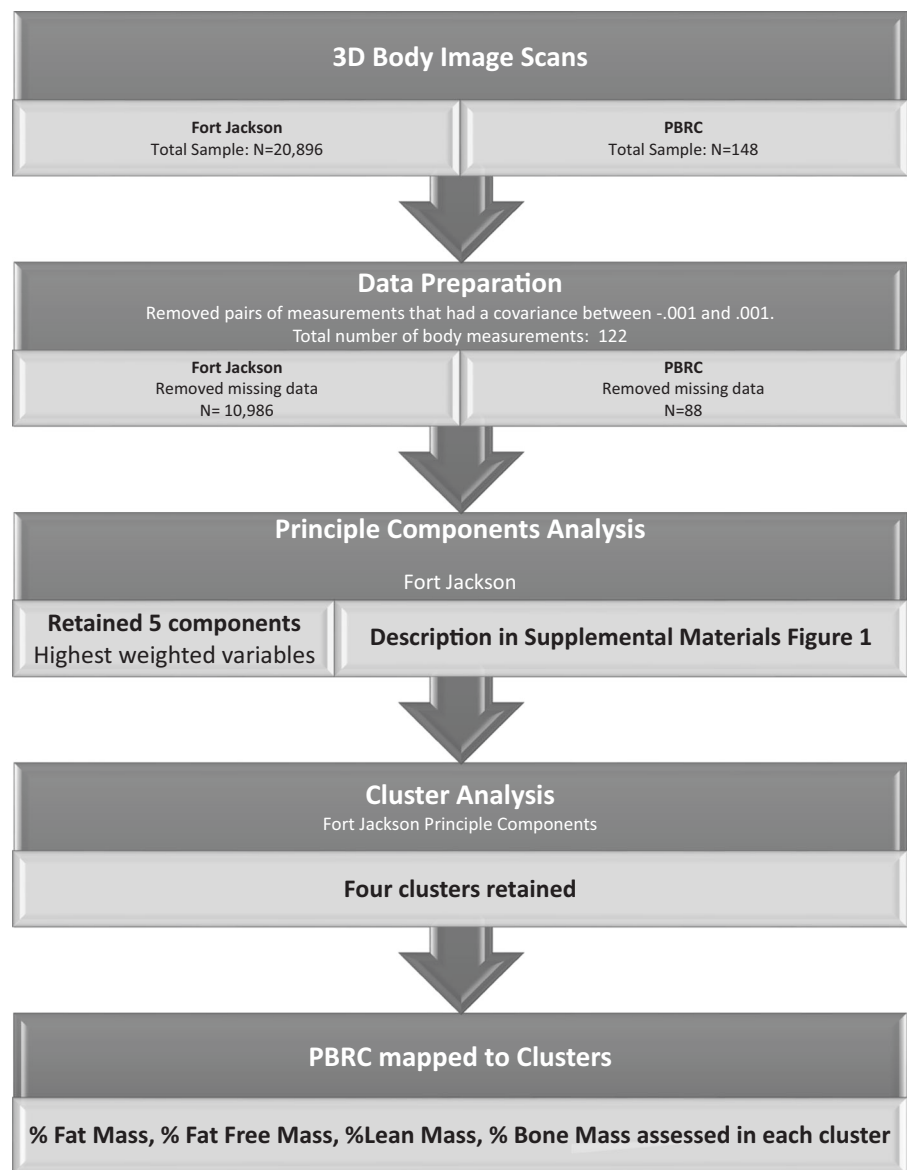
Resolution of questions 1 and 2 using machine learning requires a large and diverse population sample. To address questions 1 and 2, we used Human Solutions body scan data from over 10 000 basic training recruits assessed at Fort Jackson, South Carolina. Study design question 1 was evaluated by conducting PCA [21] on the data. After completing PCA, study design question 2 was assessed from data using a *k*-means CA [22] on the principal components previously identified in results to question 1.

Question 3 requires rigorously and carefully collected body composition data on subjects that had been simultaneously scanned using the 3D body image scanner. For this purpose, we used 3D body image scan measurements in 148 subjects obtained by the Human Solutions machine at the PBRC that also had DXA measured body composition. The principal component loadings from the Fort Jackson data were then applied to the Human Solutions measurements of the PBRC participants. After the loading, the participants from the PBRC study were assigned to clusters developed from the Fort Jackson data. The distributions of body composition within each cluster was then compared against the remaining clusters.

Subjects

Fort Jackson basic training recruits

Data from Fort Jackson, South Carolina was used to answer the first two questions in our study design. Fort Jackson currently trains 50% of the United States Army’s basic combat training load, including 60% of the female population entering the Army each year [23]. US Army basic training recruits ($N = 20\,896$ soldiers, 28% female) were scanned for uniform fitting using the 3D body imaging scanner, Human Solutions of North America (Mooresville, NC) Vitus Smart XXL 3D body scanner at Fort Jackson, SC from 1 February 2017 to 27 October 2017. Recruits were instructed on scanning posture; however, the scanning was not supervised. A database consisting of 161 anthropometric measurements per soldier, obtained from Human Solutions, was retained in spreadsheet form. Human Solutions anthropometric measurements are consistent with and have been successfully validated against research protocol manual anthropometry measurements [12, 13]. Age was not available in the database; however, basic training recruits are generally between the ages of 17 and 21 years. Individual race/ethnicity information was also not available, however, a 2010 report on overall basic training recruit

Fig. 1 Study design workflow

demographics published total recruit percentages of 18.9% black, 4.8% Asian, 0.8% Native American, and 11.9% Hispanic [24].

Pennington Biomedical Research Center

Subjects between the ages of 5 and 79 years were recruited that were of good health with an absence of major chronic diseases. Subjects were excluded if they were underweight (body mass index (BMI) < 18.5 kg/m²), over 136 kg, pregnant, had edema or dehydration. Subjects would report to PBRC to be scanned by the Human Solutions of North America (Mooresville, NC) Vitus Smart XXL 3D body scanner. Subjects also underwent a DXA scan during the same visit. Image measurements, DXA body composition data, and demographic variables were retained from adults

over the age of 18. The study was approved by the Institutional Review Board of PBRC (PBRC-12021), and all subjects signed an informed consent and Health Insurance Portability Act authorization form before participation. The study is registered on Clinicaltrials.gov (NCT02118675).

Mathematical methods

A workflow outlining mathematical procedures appears in Fig. 1. Human Solutions Fort Jackson data were first prepared for analysis, and after preprocessing, a combined PCA and CA were performed. The literature does not currently provide formal justification methods for extending a CA developed on one population to an alternate population. As a result, before extending the CA to PBRC data, we triangulated several methods that justify this extension here.

Finally, we analyze body composition in the PBRC dataset on the Fort Jackson identified clusters.

All data preparation, analysis, and modeling was performed using the statistical package R (R Core Team (2013)). Descriptive statistics were determined using the RStudio package, “psych”, and the “describe” command.

Data preparation

Missing measurements in Human Solutions data typically occur when subjects are incorrectly postured within the scanner. Because the Fort Jackson recruits were not supervised during the body scans, some recruits are missing measurements. Any recruit that was missing a measurement was removed from the database. There did not exist any missing 3D body scan body site measurements in the PBRC database, however, some subjects did not have paired DXA measurements. Only subjects that had both body scans and DXA measurements were retained.

Only one of any symmetric body measurement pairs such as left and equivalent right arm measurements were retained. This analysis was systematically performed by eliminating one of the pair of variables that had a covariance between -0.001 and 0.001 . The analysis reduced the original set of anthropometric measurements from 161 to 137 measures. This removal was performed because highly correlated variables interfere with the theoretical basis, specifically matrix formation, of the CA.

CA and PCA are sensitive to variable measures with differing units. To account for this, some preprocessing of the Fort Jackson data was done using the R package “caret” using the “preProcess” command to scale and center each of the 137 measurements [21]. The “scale” command divides each measurement value by the standard deviation of that variable. The “center” command re-centers the measurement by subtracting the variable mean from each measurement. These same preprocessing measures were then applied to the PBRC subject measurements.

Principal component analysis

Some body shape measurements are collinear. For example, height and leg length are strongly correlated. To account for these collinearities, a PCA of the Fort Jackson dataset was performed using the R package “stats”. A scree plot was formed to identify how many principal components explain an acceptable amount of variance. The first PCA did not consider gender, however a second PCA was performed that included gender as a variable. A gender-specific PCA was not performed since this would double the number of components and clusters. Separating the small sample in PBRC into these clusters would result in substantially smaller samples invalidating any potential conclusion that

could be made. Moreover, performing a gender-specific PCA would eliminate the possibility of males and females belonging to the same cluster, an outcome that carries some interesting discussion with it as to the other defining characteristics within these clusters. We preferred our analysis to allow for this possibility.

CA on the Fort Jackson study

Three different *k*-means cluster analyses were performed [22]. Each *k*-means CA was conducted using the “kmeans” package in R.

First, a *k*-means CA was performed on the first five principal components retained in the PCA (see above section). A *k*-means CA was also performed directly on the 137 different measurements obtained from Human Solutions. A final *k*-means CA was performed using only the top weighted variables in the five principal components retained in the PCA. The best CA method is the one that provides the most homogeneous clustering, which is determined by the minimal average distance over clusters from the cluster centroid to each observation within the cluster. Because many of the body shape variables are correlated, comparison of these three clustering methods used the Mahalanobis metric [25] which accounts for correlated data within the clustering algorithms.

A scree plot on the optimal cluster was formed to identify the number of clusters to retain. Four clusters were retained from the CA performed on the principal components on the Fort Jackson population sample.

Cluster assignment of the PBRC study subjects

The loading of the five principal components described above were first retained in order to assign PBRC subjects the same principal components as the ones formed by the Fort Jackson population sample. The same CA was then done on the PBRC subjects using the principal component loadings from the Fort Jackson dataset.

Extension of models from Fort Jackson to PBRC population samples

Similar to the caution required for extending a regression model beyond the population sample it was developed on, extending our analysis on the Fort Jackson population to the PBRC study needs to be justified. Unlike regression, we do not require both populations to be similar, since a CA does not rely on governing assumptions like regression does [26]. Instead we need to verify that cluster homogeneity is preserved in the second population. To preserve homogeneity across population samples, we first need to justify

applying the same loading from the PCA and then we need to confirm that homogeneity of the clusters is retained.

In order to confirm that the principal component loading structure developed on the Fort Jackson is extended to the PBRC population we need to demonstrate that the variables in both populations are similarly correlated. This was tested by evaluating the correlation of variables that yield the first principal component. Only the first principal component requires this comparison as all other principal components are orthogonal to the first.

Homogeneity of the clusters in the PBRC sample was evaluated by comparing the average Euclidean distance of each observation to its cluster center over all clusters in the Fort Jackson and PBRC datasets to determine whether the PBRC clusters were within the measured range of the Fort Jackson clusters. Specifically, the average Euclidean distance from the cluster centroid to cluster elements were computed in the Fort Jackson clusters and then compared to the analog average distances in the PBRC sample. Euclidean distance was used instead of Mahalanobis distance because the small sample in the PBRC dataset creates a singularity in its respective covariance matrix, eliminating the ability to perform Mahalanobis measurements.

Finally, similar distributions and range of body shape variables within clusters of one population sample to the other provide additional confirmation of the extension from the Fort Jackson population to the PBRC study. For example, if average and full range of BMI in the first cluster was normal for the Fort Jackson population, the average and full range of BMI should also be normal for the first cluster in the PBRC population. To this end, we calculated BMI group means and standard deviations within each cluster for both samples. We then compared the cluster-specific mean and variance for each population.

Comparison of BMI across clusters

Mean BMI values were computed for each cluster in both the Fort Jackson and PBRC datasets. Pairwise two-tailed *t*-tests of BMI were performed between each of the four clusters retained from the CA. The significance threshold was set to $P < 0.05$. Adjustments for the number of cluster comparisons were made using the Bonferroni correction ($P < 0.05/6$).

Comparison of body composition measures between clusters in the PBRC study

Percent fat mass, fat free mass, lean mass, and bone mass were computed from the DXA measurements. Mean values were calculated and then compared between clusters using two-tailed *t*-tests. Similar to the BMI comparison, the significance threshold was set to $P < 0.05$ with application of

Table 1 Subject characteristics

	Male	Female	Combined
Fort Jackson			
Age	17–21	17–21	17–21
BMI	25.60 ± 3.99	23.73 ± 2.93	25.08 ± 3.82
<i>N</i>	8717	2269	10 986
PBRC			
Age	34.5 ± 20.2	33.6 ± 17.1	34.0 ± 18.7
BMI	27.21 ± 6.44	27.96 ± 6.22	27.58 ± 6.33
<i>N</i>	45	43	88

Data are reported as mean ± SD

the Bonferroni correction adjustments for the number of cluster comparisons.

Results

Subject characteristics

After data preparation, the Fort Jackson sample contained $N = 10\,986$ subjects and PBRC consisted of $N = 88$ subjects. Descriptive statistics for the Fort Jackson and PBRC population samples appear in Table 1.

Principal component analysis

After evaluation of the PCA scree plot (Fig. 2a), we opted to retain five principal components. The highest weighted variables in each of the five principal components were Human Solutions code 9800, body weight (kg); Human Solutions code 0691, distance from the iliac crest to the floor (m); Human Solutions code 6030, distance from the narrowest part of the waist to the top of the buttocks (m); Human Solutions code 5080, distance from the narrowest part of the waist to the highest point in the buttocks (m); and Human Solutions code 0630, deviation from the narrowest part of the waist to the wall (m) (Supplemental Online Materials Fig. 1). The PCA results involving number of components and which variables held the highest weight did not alter after including gender (Supplemental Online Materials Fig. 2).

Cluster analysis

The average squared Mahalanobis distance for clustering on the five principal components was 137.99. The average squared Mahalanobis distance for clustering using only the highest weighted variables on the five principal components was 139.90. The average squared Mahalanobis distance for clustering using all 137 body measurement variables was

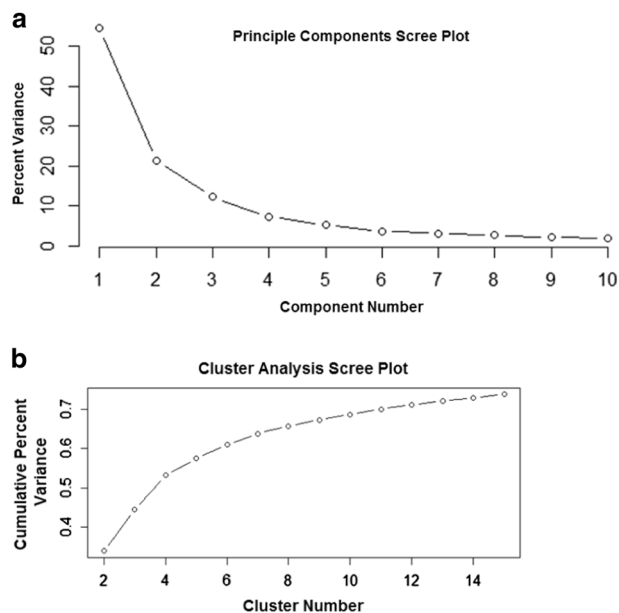


Fig. 2 Scree plots for the PCA and cluster analysis. **a** The percent of total variance explained in the Fort Jackson dataset by each principal component. The vertical axis represents the percent of the variance and the horizontal axis is the principal component number. **b** The percent of total variance in the Fort Jackson dataset that is explained with the addition of each cluster. The vertical axis represents the cumulative percent of the variance explained and the horizontal axis is the cluster number

138.01. Since clustering on the five principal components yielded the smallest average squared Mahalanobis distance, all further analysis was performed using the results of the CA on principal components.

Based on the scree plot cluster results (Fig. 2b), we selected to retain four clusters for analysis. Subject characteristics in each cluster for both the Fort Jackson and PBRC datasets appear in Table 2. Cluster-specific weight (kg), BMI (kg/m^2), and height (cm) are similar across the two datasets. Cluster 3 in the PBRC dataset has a higher percentage of females in comparison to the Fort Jackson dataset. Similar CA scree plots and cluster assignments were derived using the gender included PCA components (Supplemental Online Materials Fig. 3).

Evaluation of Fort Jackson derived principal component loadings and cluster assignments to PBRC study

Figure 3a represents a 3D plot with each cluster color-coded (cluster 1 = blue, cluster 2 = green, cluster 3 = yellow, and cluster 4 = pink) describing the relationship between the highest weighted variables in the first three principal components (Supplemental Materials Fig. 2) in the Fort Jackson dataset. The plot depicts the distinct separation of the cluster regions. Figure 3b is the analog plot for the same three

variables in the PBRC data. The range and cluster delineation in Fig. 3b is similar to the range and cluster delineation in Fig. 3a. Additionally, the points in both plots follow the same general plane indicating that the variables are correlated in the same way even though they come from two different datasets.

Average cluster-specific Euclidean distance for the Fort Jackson and PBRC datasets appear in Table 2. The PBRC dataset yielded smaller average Euclidean distance from the cluster centroid than the Fort Jackson counterpart for three of the four clusters.

Comparison of BMI across clusters

The Bonferroni correction adjustment yielded a significance threshold of $P = 0.008$. For both, the Fort Jackson and PBRC datasets, the two-sided t -test revealed that mean BMI (kg/m^2) in cluster 1 was significantly different than the mean BMI (kg/m^2) in clusters 2 and 3 ($P < 0.008$). Similarly, mean BMI (kg/m^2) was significantly different in cluster 4 when compared with clusters 2 and 3. Cluster 1 BMI (kg/m^2) was significantly different than cluster 3 BMI (kg/m^2) in the Fort Jackson sample before Bonferroni corrections ($P = 0.009$), however, did not hold after correction. Summary statistics of the pairwise t -test comparisons appear in the Supplemental Materials.

Comparison of body composition across clusters

The Bonferroni correction adjustment yielded a significance threshold of $P = 0.008$. The two-sided t -test revealed that mean percent body fat in cluster 4 was significantly different than the mean percent body fat in clusters 1–3 ($P < 0.008$). Mean percent body fat in clusters 1 and 3 differed when the significance threshold was set as 0.05, however this was not retained after Bonferroni correction. Summary statistics of the t -test comparisons appear in the Supplemental Materials.

Discussion

Human Solutions 3D body imaging and similar technology [12, 13] can automatically and accurately provide hundreds of anthropometry measurements within seconds, which presents an opportunity to predict body composition using state-of-the-art machine learning and statistical techniques. Direct prediction using standard approaches like regression depends upon research facilities to grow a database containing 3D scans and measured body composition in the same subjects. Conducting a study in this manner will take time, be expensive, and be restricted to subject samples recruited from the local vicinity of the research facility. The

Table 2 Cluster-specific subject characteristics for the Fort Jackson and PBRC studies

	Cluster 1	Cluster 2	Cluster 3	Cluster 4
Fort Jackson				
Age (years)	17–21	17–21	17–21	17–21
Height (cm)	163.02 ± 5.28	181.39 ± 5.34	171.38 ± 4.59	177.67 ± 5.01
Weight (kg)	59.61 ± 6.82	93.28 ± 9.38	76.92 ± 8.09	70.04 ± 7.03
BMI (kg/m ²)	22.95 ± 2.62	29.07 ± 3.14	26.81 ± 2.94	22.72 ± 2.28
N (% male)	2642 (29)	2404 (99)	2757 (97)	3183 (91)
Average Euclidean distance	13.01 ± 3.89	9.77 ± 2.68	9.21 ± 2.40	13.21 ± 3.28
PBRC				
Age (years)	28.73 ± 16.0	43.4 ± 16.9	39.9 ± 19.5	27.4 ± 15.4
Height (cm)	159.85 ± 7.20	178.87 ± 8.92	166.68 ± 6.31	176.28 ± 2.81
Weight (kg)	59.74 ± 8.84	100.33 ± 13.08	82.10 ± 6.23	72.33 ± 5.34
BMI (kg/m ²)	23.52 ± 3.10	31.64 ± 4.58	29.78 ± 3.86	23.28 ± 1.65
N (% male)	26 (8)	27 (81)	23 (48)	12 (92)
Average Euclidean distance	13.23 ± 3.98	9.10 ± 2.07	8.55 ± 1.46	11.93 ± 3.11
% Fat mass	31.49 ± 7.06	33.11 ± 10.46	36.46 ± 9.08	19.32 ± 7.28
% Fat free mass	69.18 ± 7.28	67.30 ± 10.99	64.03 ± 9.41	81.79 ± 7.46
% Lean mass	65.41 ± 6.98	63.80 ± 10.52	60.61 ± 9.04	77.67 ± 7.04
% Bone mass	3.76 ± 0.46	3.51 ± 0.59	3.42 ± 0.47	4.12 ± 0.47

Summary of body composition measures within each cluster for the PBRC cohort is provided. The high fat-low fat free mass group is associated with cluster number 3 while the low fat-high fat free mass group is associated with cluster number 4. Cluster number 2 represents individuals with a higher BMI and lower % fat mass than cluster number 3. Cluster number 1 is largely populated in both Fort Jackson and PBRC by females

purpose of this study was to circumvent these challenges by identifying homogenous subpopulations of 3D imaged body shapes in a large diverse dataset and pairing these findings to a smaller independent sample that contained 3D imaged body shapes with simultaneously measured body composition.

Our study reduced Human Solutions 3D body scans into four distinct subpopulations (Fig. 3) using a combined PCA and CA. The combined PCA and CA was found to be superior to using CA alone by comparison of Mahalanobis distance across each cluster. Specifically, the PCA-CA combination algorithm yielded the most homogenous clusters. Once homogenous clusters were identified, we were able to characterize these subpopulations by their body composition using data obtained at PBRC.

There were four distinct clusters that were characterized. The first can be loosely described as normal weight females, the second represents males classified with obesity with higher percent body fat, the third represents males and females classified as overweight with higher percent body fat, and the fourth as males with low percentage body fat. Interestingly, while clusters 1 and 4 did not have statistically different BMI, the two clusters did differ in percent body fat.

Our study adds to the self-organized map analysis performed on Human Solutions 3D scans by Löffler-Wirth et al. [16], which identified 13 body shape archetypes.

Because the PBRC dataset was smaller, sample sizes assigned to the 13 body shape archetypes would have resulted in even smaller sample sizes, which would have made body composition characterization prohibitive. With a larger health outcome database, a similar pairing to health outcomes could be performed as we have done here using the Löffler-Wirth body shape archetypes.

Study strengths

Nationally represented and racially diverse 3D body scan dataset

A major strength of our study was the application of Human Solutions 3D body image scans from the United States Army basic training recruits at Fort Jackson resulted in representation from every one of the 50 states of the United States. The dataset also was racially and ethnically diverse. Our dataset differs from traditional measurements collected at research sites which is restricted to subjects recruited locally.

Extension of PCA and CA to a second dataset

Special analysis had to be performed to justify the PCA-CA from Fort Jackson to the PBRC study. This is because the United States Army adheres to BMI standards that basic

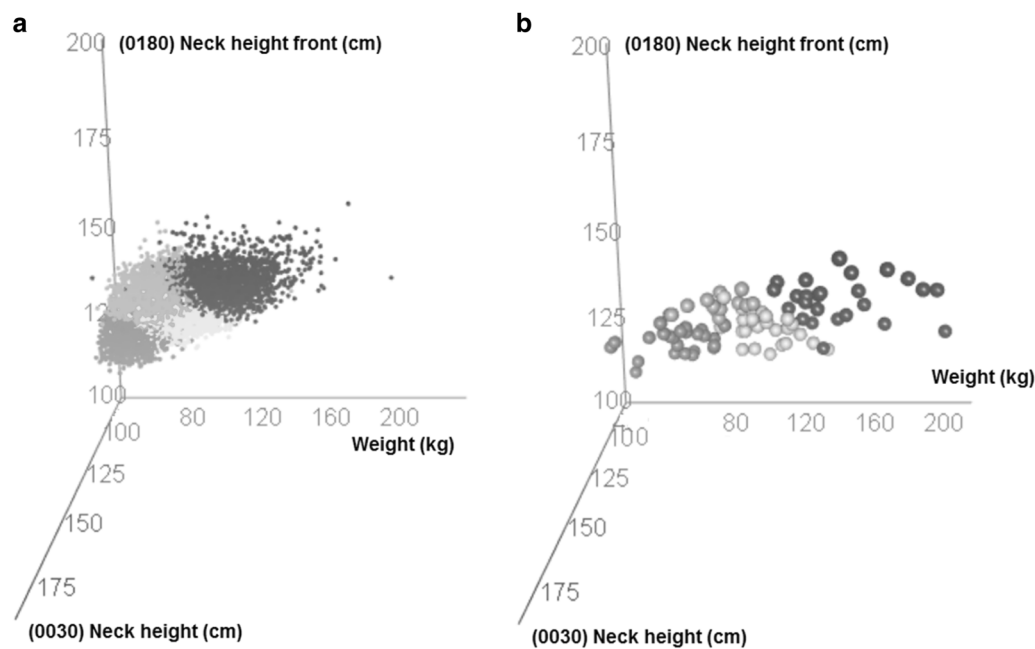


Fig. 3 Three-dimensional scatterplots of top weighted variables in the first three principal components in the Fort Jackson dataset (**a**) and the PBRC dataset (**b**). The cluster delineation and the range of data are

training recruits must satisfy in order to enlist [27]. Thus, outside a small minority of exceptions, recruits have a normal weight BMI. Moreover, basic training recruits are between the ages 17 and 21 years old. In order to extend our CA to the PBRC dataset, which contained older subjects from Baton Rouge, LA that were not held to the United States Army Body Composition standards we note several important points and justifications. First, age was not used to determine the cluster assignments in the Fort Jackson dataset. Second, the majority of the Human Solutions measurements are length measurements such as forearm length or leg length. By adulthood, these lengths are static.

However, the Human Solutions scans also contain body circumference measurements, which are highly correlated to adiposity, which are a function of age [5, 28]. The justification for extending the conclusions was supported by similar BMI distributions within clusters between the two datasets. By computing ranges and distances, we also found that cluster homogeneity was preserved across the two datasets. Future studies that choose to employ the pairing application we have performed here can apply the same process to justify such an extension.

Study limitations

Our study has several limitations. First, the PBRC population sample is small. This limited our ability to separate the population by gender in the PCA and to consider more clusters. As more data are acquired at different sites that are

similar in both plots. The axis label descriptions relying on Human Solutions measurements (neck height and neck height front) appear in Supplemental Materials Fig. 2

using the Human Solutions technology, we anticipate a more robust analysis within clusters.

Second, any analysis that is dependent on one type of machine, for example, Human Solutions, is restricted to the specific machine. There are many new and advancing 3D body image scanning technologies that are rapidly becoming available. Some of the technologies are cheaper and available for individual consumers using smart phones [29–31] while others are more sophisticated and focus on accuracy and rapid image acquisition. It is unlikely that the measurements or image quality will ever be standardized. Therefore, either individual technology specific studies analyzing data would need to be performed as we and others have done [16] or a partial automatic analysis software analysis could be made available.

Because the analysis presented here is not readily tractable, delivering the final predictions for direct clinical applications also represents a challenge. We advocate for programming predictions directly in the Human Solutions device so that outcomes can be provided directly upon scan.

Conclusions

3D body scan image data offers a wealth of human anthropometric data that can be quickly and accurately obtained in large populations. A CA can pair these large datasets to health outcomes that are difficult to collect from smaller sized datasets. The results of these analyses can be clinically deployed in either software or directly within the 3D scanning device.

Acknowledgements

Funding: This work was partially supported by two National Institutes of Health NORC Center Grants P30DK072476, Pennington/Louisiana; and P30DK040561, Harvard; and R01DK109008, Shape UP! Adults.

Compliance with ethical standards

Conflict of interest The authors declare that they have no conflict of interest.

References

- Dublin LI, Lotka AJ, Metropolitan Life Insurance Company, Statistical Bureau, Metropolitan Life Insurance Company. Twenty-five years of health progress; a study of the mortality experience among the industrial policyholders of the Metropolitan Life Insurance Company 1911 to 1935. New York, San Francisco: Metropolitan Life Insurance Company; 1937. xi, p. 611 (incl. illus. (maps) tables, diagrs).
- Heo M, Kabat GC, Gallagher D, Heymsfield SB, Rohan TE. Optimal scaling of weight and waist circumference to height for maximal association with DXA-measured total body fat mass by sex, age and race/ethnicity. *Int J Obes (Lond)*. 2013;37:1154–60.
- Heymsfield SB, Chiracharyavej T, Rhyu IJ, Roongpisuthipong C, Heo M, Pietrobello A. Differences between brain mass and body weight scaling to height: potential mechanism of reduced mass-specific resting energy expenditure of taller adults. *J Appl Physiol* (1985). 2009;106:40–8.
- Heymsfield SB, Peterson CM, Thomas DM, Heo M, Schuna JM Jr., Hong S, et al. Scaling of adult body weight to height across sex and race/ethnic groups: relevance to BMI. *Am J Clin Nutr*. 2014;100:1455–61.
- Bouchard C. BMI, fat mass, abdominal adiposity and visceral fat: where is the 'beef'? *Int J Obes (Lond)*. 2007;31:1552–3.
- Motamed N, Rabiee B, Hemasi GR, Ajdarkosh H, Khonsari MR, Maadi M, et al. Body roundness index and waist-to-height ratio are strongly associated with non-alcoholic fatty liver disease: a population-based study. *Hepat Mon*. 2016;16:e39575.
- Tian S, Zhang X, Xu Y, Dong H. Feasibility of body roundness index for identifying a clustering of cardiometabolic abnormalities compared to BMI, waist circumference and other anthropometric indices: the China Health and Nutrition Survey 2008 to 2009. *Medicine (Baltimore)*. 2016;95:e4642.
- Maessen MF, Eijssvogels TM, Verheggen RJ, Hopman MT, Verbeek AL, de Vegt F. Entering a new era of body indices: the feasibility of a body shape index and body roundness index to identify cardiovascular health status. *PLoS ONE*. 2014;9:e107212.
- The National Health and Nutrition Examination Survey (NHANES) Anthropometry Procedures Manual. CDC. CfDC January 2007. <https://www.cdc.gov/nchs/data/nhanes3/manuals/anthro.pdf>.
- Nordhamm K, Sodergren E, Olsson E, Karlstrom B, Vessby B, Berglund L. Reliability of anthropometric measurements in overweight and lean subjects: consequences for correlations between anthropometric and other variables. *Int J Obes Relat Metab Disord*. 2000;24:652–7.
- Wang J, Bartsch G, Rahgavan SS, Yurik T, Peng G, Chen L, et al. Reliability of body circumference and skinfold measurements by observers trained in groups. *Int J Body Comp Res*. 2004;2:31–6.
- Kuehnappel A, Ahnert P, Loeffler M, Broda A, Scholz M. Reliability of 3D laser-based anthropometry and comparison with classical anthropometry. *Sci Rep*. 2016;6:26672.
- Soileau L, Bautista D, Johnson C, Gao C, Zhang K, Li X, et al. Automated anthropometric phenotyping with novel Kinect-based three-dimensional imaging method: comparison with a reference laser imaging system. *Eur J Clin Nutr*. 2016;70:475–81.
- Koepke N, Zwahlen M, Wells JC, Bender N, Henneberg M, Ruhli FJ, et al. Comparison of 3D laser-based photonic scans and manual anthropometric measurements of body size and shape in a validation study of 123 young Swiss men. *PeerJ*. 2017;5:e2980.
- Stewart AD, Klein S, Young J, Simpson S, Lee AJ, Harrild K, et al. Body image, shape, and volumetric assessments using 3D whole body laser scanning and 2D digital photography in females with a diagnosed eating disorder: preliminary novel findings. *Br J Psychol*. 2012;103:183–202.
- Löffler-Wirth H, Willscher E, Ahnert P, Wirkner K, Engel C, Loeffler M, et al. Novel anthropometry based on 3D-bodyscans applied to a large population based cohort. *PLoS ONE*. 2016;11:e0159887.
- Reynolds G, Shendruk A. Demographics of the U.S. Military: Council on Foreign Relations. 2018. <https://www.cfr.org/article/demographics-us-military>.
- Army Demographics FY16 Profile. 2016. https://m.goarmy.com/content/dam/goarmy/downloaded_assets/pdfs/advocates-demographics.pdf.
- Yun DJ, Yun DK, Chang YY, Lim SW, Lee MK, Kim SY. Correlations among height, leg length and arm span in growing Korean children. *Ann Hum Biol*. 1995;22:443–58.
- Bogin B, Varela-Silva MI. Leg length, body proportion, and health: a review with a note on beauty. *Int J Environ Res Public Health*. 2010;7:1047–75.
- Jolliffe IT. Principal component analysis. 2nd ed. New York: Springer; 2002. xxix, p. 487.
- DeGregory KW, Kuiper P, DeSilvio T, Pleuss JD, Miller R, Roginski JW, et al. A review of machine learning in obesity. *Obes Rev*. 2018;19:668–85.
- US Army Training Center, Fort Jackson. 2018. <http://jackson.armylive.dodlive.mil/about/>. Accessed on 14 June 2018.
- Military Recruitment 2010. National Priorities Project. 2011. <https://www.nationalpriorities.org/analysis/2011/military-recruitment-2010/>. Accessed on 14 June 2018.
- Varmuza K, Filzmoser P. Introduction to multivariate statistical analysis in chemometrics. Boca Raton: CRC Press; 2009. xiii, p. 321.
- Freedman D, Pisani R, Purves R. Statistics. 4th ed. New York: W. W. Norton & Co.; 2007.
- Army Regulation 600-9. The army body composition program. In: DoD, editor. Washington DC: The Department of the Army; 2013.
- Gallagher D, Heymsfield SB, Heo M, Jebb SA, Murgatroyd PR, Sakamoto Y. Healthy percentage body fat ranges: an approach for developing guidelines based on body mass index. *Am J Clin Nutr*. 2000;72:694–701.
- Heymsfield SB, Bourgeois B, Ng BK, Sommer MJ, Li X, Shepherd JA. Digital anthropometry: a critical review. *Eur J Clin Nutr*. 2018;72:680–7.
- Bourgeois B, Ng BK, Latimer D, Stannard CR, Romeo L, Li X, et al. Clinically applicable optical imaging technology for body size and shape analysis: comparison of systems differing in design. *Eur J Clin Nutr*. 2017;71:1329–35.
- Pradhan L, Song G, Zhang C, Gower B, Heymsfield S, Allison D, et al. editors. Feature extraction from 2D images for body composition analysis. IEEE International Symposium on Multimedia (ISM). Miami, FL, USA: IEEE; 2015.